World Academy of Science, Engineering and Technology
International Journal of Electrical and Computer Engineering
Vol:6, No:2, 2012

An Advanced Time-Frequency Domain Method for PD Extraction with Non-Intrusive Measurement

Guomin Luo, Daming Zhang, Yong Kwee Koh, Kim Teck Ng, Helmi Kurniawan, and Weng Hoe Leong

***Abstract*—**Partial discharge (PD) detection is an important method to evaluate the insulation condition of metal-clad apparatus. Non-intrusive sensors which are easy to install and have no interruptions on operation are preferred in onsite PD detection. However, it often lacks of accuracy due to the interferences in PD signals. In this paper a novel PD extraction method that uses frequency analysis and entropy based time-frequency (TF) analysis is introduced. The repetitive pulses from convertor are first removed via frequency analysis. Then, the relative entropy and relative peak-frequency of each pulse (i.e. time-indexed vector TF spectrum) are calculated and all pulses with similar parameters are grouped. According to the characteristics of non-intrusive sensor and the frequency distribution of PDs, the pulses of PD and interferences are separated. Finally the PD signal and interferences are recovered via inverse TF transform. The de-noised result of noisy PD data demonstrates that the combination of frequency and time-frequency techniques can discriminate PDs from interferences with various frequency distributions.

***Keywords*—**Entropy, Fourier analysis, non-intrusive measurement, time-frequency analysis, partial discharge

I. Introduction

DETECTING and identifying partial discharges (PDs) in metal-clad apparatus such as gas or oil insulated switchgear and transformers are well-established procedures[1]. In traditional methods, the PD sensors are mounted inside the metallic enclosure which promises high signal to noise ratio (SNR). But for operational switchgears and transformers without such PD sensors, arranging a shutdown specifically to fit internal couplers rarely can be justified[1]. So external non-intrusive sensors which are easy to install and have no interruptions on operation are becoming more and more popular for the devices which are not suitable to install internal sensors. Usually, the radiating electromagnetic wave from PD source escapes out of the cracks on switchgear and transformer enclosure and forms a small pulse-like voltage on the metal tank surface. This is so called transient earth voltage (TEV)[2],[3]. The non-intrusive PD sensors detect those impulsive TEV signals to determine the existence of PD.

Guomin Luo is with Nanyang Technological University, Singapore. (e-mail: luog0003@e.ntu.edu.sg).

Daming Zhang was with Nanyang Technological University. He is now with School of Electrical Engineering and Telecommunication, University of New South Wales, Sydney. (e-mail: daming.zhang@unsw.edu.au).

Mr YongKwee Koh, Mr KimTeck Ng, Mr Helmi Kurniawan and Mr WengHoe Leong are with Hoestar Inspection International Pte Ltd., Singapore.

When detecting PDs on the external surface of enclosure, one of the major problems that need to be addressed is the interferences from surroundings.

Some hardware solutions such as non-intrusive sensors shielded with metal cover have been proposed to eliminate noises. Besides hardware design and improvement, the signal processing based noise-rejection is also a powerful tool to reject noises in measured PD signals with much lower costs. The time-domain features such as pulse height and phase angle, as well as the frequency-domain features such as frequency distribution, are often used to discriminate PDs from noises[4]. Meanwhile, the time-frequency (TF) analysis and artificial intelligence are also utilized[5]-[7].

All these approaches have pros and cons. The time-domain or frequency-domain algorithms are simple, fast, and easy to realize. But they have drawbacks when used to distinguish pulses with similar features. For instance, it is very hard for time-domain analysis which only reflects time-domain features to discriminate PD and impulsive noise if two pulses occur at the same time. This is also true for frequency-domain methods when the frequency ranges of PD and pulses overlap with each others. Therefore, time-frequency analysis which reveals the energy variation with both time and frequency was proposed. However, separation of pulses occurring at same time and having same frequency range is still a question. Meanwhile, how to extract PDs from the TF spectrum remains a big challenge. Artificial intelligence based methods such as neural network and fuzzy logic have also been employed. However, the large database that is needed in training is usually difficult to collect in most field tests. Therefore, all these approaches are good at removing particular kinds of noises. Any method alone may not produce good results in rejecting all noises in on-site PD measurement. Combination of the signal processing methods in different domains is a potential way to extract PDs from noisy background.This paper proposes a novel PD extracting method which, based on frequency distribution, groups the pulses with similar features and reject noise according to the PD characteristics. This paper begins with the fundamentals of non-intrusive measurement. Then, the features of noises and possible rejecting methods are discussed. Next, an advanced PD extracting method is introduced and the details of its algorithm are analyzed. Finally, this PD extracting method is performed on a noisy PD signal to demonstrate its effectiveness in noise rejection.

II. Measurement Setup

When PD occurs in electrical apparatus, there is a voltage induced on its grounded or earthed metallic enclosure. To illustrate this idea, a laboratory test is set up as shown in Fig.1, where a PD generator is placed inside a metallic enclosure. The PD signals are recorded using an oscilloscope. (Tektronix TDS7104, band width: up to 1GHz and sampling rate: up to 10GHz/s).

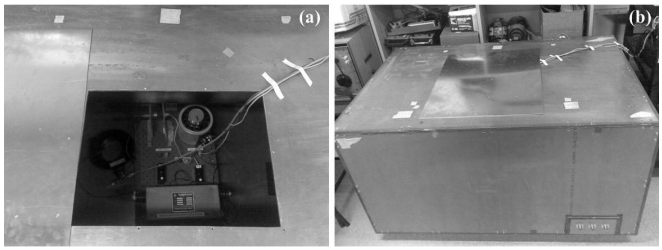

Fig. 1 PD generator placed inside a metallic enclosure: (a) enclosure with its cover open, (b) enclosure with its cover close

A. PD Sensor

Fig.2 shows the drawing of the developed coaxial sensor for non-intrusive PD measurement with protruding inner conductor (part 4) extending beyond the bottom of outer conductor (part 3). Part 1 is the female BNC interface and it is integrated with part 2.

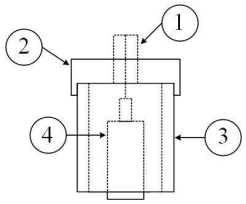

Fig. 2 Coaxial PD sensor

Since the electrical apparatus are located inside a metal cladding, the high frequency components of the PDs emerging in the apparatus attenuate greatly through propagation. The high-frequency energy of most PDs detected on the outside surface cannot be greater than low frequency part unless a high-frequency amplifier is added. Therefore, the PD sensor for non-intrusive measurement should have a frequency response range wide enough to capture PD energies as much as possible and a lower-cutoff frequency small enough to ensure the less-distorted low-frequency energy are recorded.

As an important factor, the amplitude response of the coaxial sensor is shown in Fig.3.

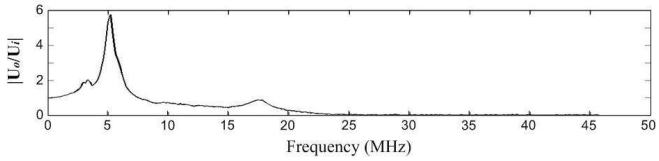

Fig. 3 Amplitude response of the coaxial sensor

Here, $|U_o/U_i|$ equals to the absolute value of output voltage divided by input voltage at different frequencies. The -3dB point is around 80Hz at low frequency side and around 9MHz at high frequency side. The -3dB point is defined as the frequency where $20\log_{10}|U_o/U_i|$ equals -3.

B. PD Features with Non-Intrusive Measurement

In Fig. 1(a), besides the PD generator, there is also a HFCT placed inside the metallic cavity. Using the two similar coaxial sensors as shown in Fig. 2 and the HFCT, PD measurement was carried out in our laboratory. The sensor placed outside and on top of the metallic enclosure has its part 4 or inner electrode electrically contact with the outer surface of the top of the metallic enclosure. Similarly the sensor placed inside the metallic enclosure has its part 4 electrically contact with the interior surface of the bottom of the metallic enclosure. The results are shown in Fig.4 for two different durations, where the top wave is measured PD pulses using HFCT; the middle wave is data from the sensor placed inside the enclosure; the bottom wave is output from the sensor placed outside the enclosure. From these two figures, one can see that the measured PD pulses are almost the same from the two coaxial sensors placed inside and outside the metallic enclosure. Thus one can conclude that when PD occurs inside the enclosed metallic cavity, there is an induced voltage on its interior metallic surface, which is almost equally measurable by the sensor placed outside it. This provides fundamental basis for field test of metal-clad apparatus using non-intrusive PD sensing technique.

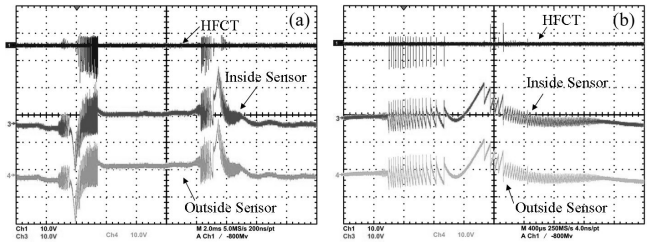

Fig. 4 Measured PD pulses with different durations, (a) PDs of a power frequency cycle (20 milliseconds), (b) PDs of 4 milliseconds

The frequency distribution of signal collected by coaxial sensor is generated by Fourier transform and shown in Fig.5.

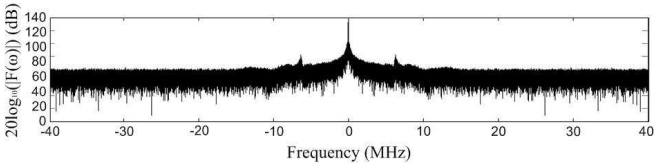

Fig. 5 Frequency distribution of signal in Fig.4(b)

If Fig.5, $20\log_{10}(|F(\omega)|)$ values are plotted to give a clear understanding. Here, $|F(\omega)|$ is the Fourier transform of signal f in Fig.4(b), ω denotes the frequency. The higher frequency range such as 30MHz that goes beyond the signal capture capability of coaxial sensor could be assumed to be dominated by white noise. Then, the noise level in Fig.5 is around 60dB which equals to the values of frequency distribution higher than

30MHz. The PD energies greater than this noise level are concentrated below 15MHz.

III. Noise Types And Features

Noise can be due to several kinds of sources and can couple with the systems in different ways and with different features. Therefore, noise rejection has no omnipotent solution and is best approached by devising several techniques, each of them tailored for a specific kind of noise[8]. To develop suitable tools for each kind of noise, the noise types and features are analyzed. Much previous work and field tests suggests that the noises that most likely need to be rejected during on-site measurements of metal-clad apparatus are: white noise, harmonics, repetitive pulses and random pulses[9]. Those noises have different patterns and can be classified into two groups: non-impulsive interferences and impulsive interferences. Features and potential rejections of these two groups of interferences are introduced in detail in following paragraphs.

A. Non-Impulsive Interferences

Non-impulsive interferences include white noise and sinusoidal noises.

White noises are the most common background noise. They are usually generated by amplifier, oscilloscope or any electrical equipment. White noises are equal-power signals. They have equal power density throughout the whole frequency range.

The harmonic signals usually come from communication systems or electronics equipments. They contain same frequency components throughout all time. Their energy decreases greatly in the frequency range that does not equal to their oscillating frequencies. Therefore, they appear to be sharp singularities in frequency domain or time-axis-paralleling strips in time-frequency domain.

Commonly, the white noise and harmonics can be rejected by frequency-dependent thresholding. Both of them are very easy to remove when comparing with impulsive interferences.

B. Impulsive Interferences

Impulsive interferences usually include repetitive pulses and random pulses. Impulsive disturbance is difficult to distinguish by using only one technique because of its similarity with PD pulses in some aspects. The methods such as thresholding which is effective to remove white noise and harmonics are often ineffective to remove pulse-like disturbances. Therefore, advanced method should be explored.

Repetitive pulses usually come from electronics apparatus such as AC/DC convertor and rectifier. The repetitive pulses from same source must have same features (i.e. frequency distribution). Meanwhile, because of the regular switching behaviors of electronics equipment, the repetitive pulses tend to group at equally-spaced phase values. Highly-repetitive occurrence of these exactly same and equally-spaced pulses can produce large-amplitude singularities in frequency domain. This characteristic suggests a possible solution of repetitive impulsive noise in frequency domain. Furthermore, the frequency-domain method is possible to separate pulses occurring concurrently.

Besides the repetitive pulses from electronics equipment, random pulse is another type of impulsive interference that is often encountered in field test. Random pulses come from switching operations, lightning and so on. In general, there is not any correlation between supply voltage wave and random pulses, and the random pulses from the same source are not identical at different time moments. Thus, unlike repetitive pulses, the large-amplitude singularities in frequency-domain which are caused by repetitive occurrence of same pulses are seldom found in the frequency domain of random pulses. It is very hard to discriminate PDs from random pulses via frequency-domain analysis. However, the frequency distributions of pulses from the same source must be highly similar and different from those of pulses from other sources. For example, the PD pulses from the same source that travel along the same path should have identical distortion during propagation. Their frequency distributions must be different with those of pulses that happen in the immediate vicinity of PD sensor which means less distortion. This difference in frequency distribution of each pulse suggests that the PDs and noises can be classified and recognized pulse-by-pulse according to their frequency distributions. Time-frequency analysis is an efficient tool that reveals the frequency distribution of each pulse if the parameters are selected appropriately. It could be a potential solution of grouping pulses with similar frequency distributions.

IV. Processing System

The noise rejecting method proposed here is mainly based on frequency distributions of PD and noises. Referring to the analysis of noises in section III, the non-impulsive noises can be rejected via thresholding, the repetitive pulses can be removed by frequency analysis and the random pulses can be classified by their time-frequency distributions. Therefore, three main steps are included in this de-noising method: pre-processing, TF feature extraction, and pulse extraction. Here, TF feature extraction and pulse extraction are combined to be PD extraction. The flowchart in Fig.6 illustrates the procedure of processing system.

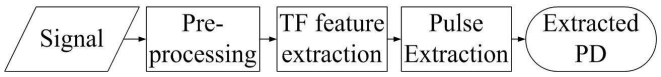

Fig. 6 Flowchart of the processing system

A. Pre-processing

Pre-processing is based on frequency-domain analysis. The repetitive pulses and harmonics that have large-energy in frequency domain are removed by this step. As mentioned in section III, harmonics and repetitive pulse can produce large-amplitude singularities in frequency domain. On the other hand, PD is a random phenomenon and cannot generate large-amplitude singularities in frequency domain. Therefore, the large-amplitude singularities in frequency domain can be

regarded as noise-related energies. In this proposed method, the frequency distribution of whole signal is generated via Fourier transform and the large-amplitude singularities are removed. In most cases, the highly-repetitive pulses can be removed in pre-processing.

B. PD Extraction

After pre-processing, which rejects most repetitive pulses in noisy data, the frequency distribution of each pulse is generated by time-frequency analysis. Here, short-time Fourier transform (STFT) is employed. The size of sliding window is selected to be the duration of longest pulse in noisy signal to ensure the whole frequency distribution of a single pulse is included in one time-indexed vector in TF spectrum. Therefore, each time-indexed vector in TF spectrum is analyzed and classified. Two parameters: relative entropy and relative peak-frequency are employed to describe the frequency distribution of each time-indexed vector. Pulses with similar parameters are clustered and classified. Finally, based on PD feature analysis, the noises are rejected and PD pulses are retained.

V. PRE-PROCESSING

As mentioned in section III, repetitive pulses from the same source should have the same characteristics. Highly-repetitive occurrence of these identical and equally-spaced pulses can produce large-amplitude singularities in frequency domain. Fig.7 gives an example to demonstrate this phenomenon. This repetitive pulse signal is generated by a high-frequency PFC (power factor correction) convertor in laboratory and detected by coaxial sensor in Fig.2.

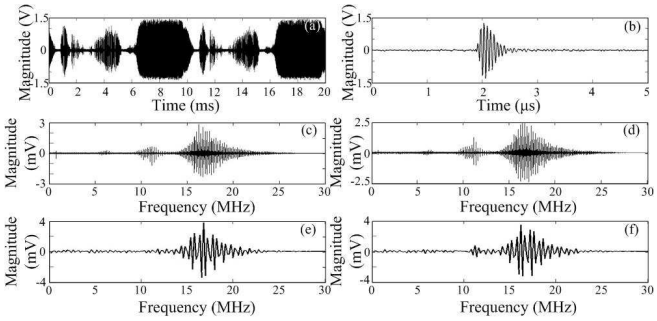

Fig. 7 The Fourier coefficients of repetitive pulses of one cycle and a single pulse, (a) noise of one cycle, (b) single noise pulse,(c) the real Fourier coefficients of signal in (a), (d) the imaginary Fourier coefficients of signal in (a), (e) the real Fourier coefficients of pulse in (d), (f) the imaginary Fourier coefficients of pulse in (d)

Fig.7 shows most energy of single noise pulse is in the frequency band from 15MHz to 20MHz. This is consistent with the energy distribution of pulse group of one cycle. Meanwhile, the amplitude of Fourier coefficients decreases greatly if the frequency does not correspond to the peak frequencies.

According to this characteristic of repetitive pulses, a Fourier coefficients based noise reduction method is proposed as follow: First, the real and imaginary Fourier coefficients of noisy data are produced by Fourier transform. In order to keep the smooth energy in Fourier coefficients, the frequency axis is divided into many small frequency bands. Each band has a bandwidth of 0.5MHz. An empirical threshold 8σ is applied and moving along the frequency axis to detect the singular points in each frequency band. Here, σ is the estimation of white noise. Theoretically, setting the singular coefficients to zero could totally remove the periodic energy. But in practical application, the nearby coefficients of singular points also have large amplitude. A filter [1, 1-1/n, …, 1/n, 0, 1/n, …, 1-1/n, 1] is thus employed, where $2n+1$ is the width of filter. The filter's shape looks like an inverted triangular. By filtering the singular points with this inverted triangular filter, the coefficients near the singularities can also be reduced.

VI. PD EXTRACTION

A. Pulse Features Extraction

In order to extract PD pulses effectively and automatically, the features of frequency distributions need to be extracted. The extracted features must be independent of shift, polarity, amplitude, and sampling points. These requirements suggest that the PD pulses from the same source with different phase angles, magnitude, and sampling rates should have similar features. The requirements can be satisfied by using relative entropy and relative peak-frequency which are calculated with normalized TF spectrum.

In this paper, the TF spectrum is generated by short-time Fourier transform (STFT). It has often been used to determine the sinusoidal frequency components and phase features of local sections of signal. For any signal f, the resulting STFT is as follow:

$$Sf(u,\xi) = \left\langle f, g_{u,\xi} \right\rangle = \int_{-\infty}^{+\infty} f(t) g(t-u) e^{-i\xi t} dt \qquad (1)$$

The sliding window $g_{u,\xi}(t)=e^{i\xi t}g(t-u)$ is a real and symmetric window $g(t)=g(-t)$, translated by u and modulated by the frequency ξ. It is normalized $\|g\|=1$, so that $\|g_{u,\xi}\|=1$ for any real numbers u and ξ.

PD pulses have a quite short duration and wide frequency range[10]. Empirically, a window with larger bandwidth and rapid decay is better for TF analysis of PD signal. The hanning window is thus selected. In order to keep enough frequency resolution and ensure whole frequency distribution being contained in one time-indexed vector, the size of window $g(t)$ is defined

$$K = \begin{cases} \max\{|K|_{K\in Z}, K \geq L, K/2 \mod N\}, & if \quad L \geq 2\ \mu s \\ 2\ \mu s, & if \quad L < 2\ \mu s \end{cases} \qquad (2)$$

where, L is the length of pulse with longest duration in noisy PD data F, N is the length of F. When the longest duration L of pulse is greater than 2 microseconds, the window size K is the smallest integer that satisfies $K \geq L$ and $K/2$ divides N. If L is shorter than 2 microseconds, the window size K is set to 2 microseconds to promise enough resolution in frequency.

When the window $g(t)$ slides along the time axis, the frequency spectrum of the windowed signal is revealed. The spectrum of the whole time range forms a two-dimensional representation of signal which is called time-frequency spectrum[11]. It is denoted P_s:

$$P_S f(u,\xi) = |Sf(u,\xi)| \tag{3}$$

From the definition of TF spectrum, one can easily find whole frequency distribution of single pulse is contained in one time-indexed TF vector. This time-indexed frequency distribution is independent of the polarity and phase angle of pulses.

The time-indexed vector in TF spectrum is actually the energy distribution of pulse in TF domain. Its coefficients vary a lot with frequency. To produce a feature unaffected by magnitude, normalization of TF spectrum is applied as follows: the TF spectrum indexed by each frequency is subtracted by its minimum value and then is divided by its maximum value. Thus, in normalized TF spectrum, the minimum and maximum value in whole TF spectrum is 0 and 1, respectively. However, in this normalized TF spectrum, the influence from noises, especially white noise, cannot be ignored because the differences between pulse and noise coefficients decrease greatly. Thus, to eliminate the influence from white noise, the smaller coefficients in each frequency are removed by a threshold. To select as much large-amplitude coefficients as possible, a threshold with smallest estimation risk is needed. The minimax estimation which has been proved to have a smaller estimation risk than most other thresholding techniques is provided in [12], which uses a threshold to yield minimax performance for mean square error against an ideal procedure. For easy application in program design, an approximate minimax estimator can be used[13]. The threshold λ equals:

$$\lambda = \begin{cases} 0 & (m \le 32) \\ \varepsilon * (0.3936 + 0.1829 * \log_2 m) & (m > 32) \end{cases} \tag{4}$$

where m is the length of time scale and $m=N/M$, ε is the estimated variance of noise. As white noise of each frequency follows Gaussian distribution, the estimated variance of Gaussian noise was proved to be $\varepsilon \approx M_X/0.6745$ where M_X is the median of absolute coefficients. The coefficients larger than threshold are regarded to contain pulse energy.

After normalization and thresholding, the time-indexed vectors in revised TF spectrum denote the relative frequency distributions of all pulses. This relative frequency distribution satisfies all the requirements of features such as independent of shift, polarity, amplitude, and sampling points. However, in order to discriminate PD pulses from noises automatically, parameters that can describe this relative frequency distribution are needed. Therefore, relative entropy σ_E and relative peak-frequency σ_F are proposed.

1) Relative Entropy

Entropy is a measure of disorder. Here, the entropy means Shannon Entropy. The more chaotic signal must generate greater entropy. That means the time-indexed vector which has more varying coefficients will generate larger entropy value. The entropy H of each time-indexed vector X with possible values $\{x_1, x_2, \ldots, x_n\}$ is defined as follow[14]:

$$H(X) = -\sum_{i=1}^{n} p(x_i) \log_b p(x_i), \tag{5}$$

where $p(x_i)$ is the probability of x_i, and b is the base of logarithm. Common value of b is 2, and the unit of entropy is bit.

From (5), we can conclude that the value of $H(X)$ depends on the size of time-indexed vector X. In order to eliminate the influence from size, the relative entropy σ_E which equals the ratio of entropy value of each time-indexed vector to the maximum entropy of X is proposed. As shown in (5), entropy value $H(X)$ reaches its maximum when all probabilities $p(x_i)$ are equal, $p(x_1)=p(x_2)=\ldots=p(x_n)=1/n$, and $H(X)_{\max}=\log_b n$, where n is the size of X. Thus, the related entropy σ_E is defined as:

$$\sigma_E = H(X)/H(X)_{\max} \tag{6}$$

The relative entropy only reflects the relative disorder of frequency distribution of each pulse. It is independent on the size of vector X. That is to say this relative entropy is independent on the sampling rate and size of sliding window. The pulses of the same type which have similar frequency distribution should have similar relative entropy.

2) Relative Peak-Frequency

Since the relative entropy of time-indexed TF spectrum is a measure of chaotic distribution, pulses with different distribution but similar disorder may have similar entropy. However, if two pulses from different sources have similar relative entropy values, their frequencies with largest energy cannot be the same because of their different frequency distributions. Therefore, the location of peak-frequency or the frequency of largest energy in each time-indexed vector X is employed in classification. Similarly, in order to eliminate the influence from size of X, the relative peak-frequency σ_F is defined

$$\sigma_F = F(X)/F_{\max} \tag{7}$$

Here, $F(X)$ is the frequency with maximum energy in time-indexed vector X, $F_{\max}$ is the size of X which is half of the sampling rate. As a parameter that describes relative location of peaks in frequency distributions, relative peak-frequency σ_F also satisfies independency requirements mentioned before.

B. PD Pulse Extraction

PD pulse extracting algorithm groups the pulses with similar parameters at first and then extracts the group or groups with most similar features with PDs. Therefore, PD pulse extracting method includes two steps: pulse grouping and noise rejection.

1) Pulse Grouping

As discussed in section VI.A, two parameters: relative entropy σ_E and relative peak-frequency σ_F are used to describe the frequency distribution of each time-indexed vector which contains whole information of each pulse. The vectors with similar parameters σ_E and σ_F are grouped in this step. In practical application, pulse grouping should be fast and be able to deal with complex situations such as large number of pulses.

Clustering analysis was proved to be effective in grouping data[8]. The distance between two points are calculated and compared. The points are grouped if the distance between them is small and separated if the distance is large. Usually, clustering analysis is a time-consuming procedure since the distances between every two points should be calculated.

However, because only two parameters: relative entropy σ_E and relative peak-frequency σ_F are employed in this proposed method, the points near to each others should have similar values of both σ_E and σ_F. Therefore, the two parameters are first grouped respectively. For any one-dimensional vector, the points that belong to the same group must be close to each others and gather around their center. Between two groups, there must be a boundary where the number of points is very small. If the value range of σ_E or σ_F is divided into many intervals such as ten intervals, the histogram which denotes the number of points of each interval reveals the density of points. Maxima in histogram suggest centers of groups and minima suggest boundaries. Finding all the boundaries in σ_E and σ_F can divide the zones of clustered groups in σ_E-σ_F plane. For example, if there are two minima in histogram of σ_E and one minimum of σ_F, three and two segments are divided in σ_E and σ_F, respectively. Then six groups can be clustered in σ_E-σ_F plane. Although the gathering results have little differences with the one generated by ordinary clustering analysis, the difference should not be great as only two parameters are included. Meanwhile, this method is much faster.

2) PD reorganization

In non-intrusive measurement, the PD signal occurs inside the cladding has to travel a long way before being captured by PD sensors. Because their high-frequency energy decreases greatly during propagation, the relative peak-frequency σ_F of PD pulses should be smaller than impulsive noises which often have large oscillating components. On the other hand, the PD pulses usually have short duration and wide frequency range. That means, after thresholding, more coefficients with different amplitudes are contained in the time-indexed vector of PD pulse than those of other impulsive noises. The relative entropy σ_E of PD-contained time-indexed vector is thus larger. Therefore, the pulse groups with larger σ_E and smaller σ_F can be classified as PD.

VII. Case Study

The results and procedure of processing a combined signal with proposed method are reported in the following content as an example.

The combined signal is made of a field-collected noise and a laboratory-generated PD data. Both signals are detected by the coaxial sensor in Fig.2. The PD signal is detected on the outside surface of metallic enclosure. The noise data is collected on the external surface of a gas-insulated switchgear. The field-collected noise data contains several kinds of impulsive interferences from convertors. Since large differences exist between the magnitudes of laboratory and field collected signals, the latter one is amplified before adding to the PD signal.

The original data and the results after pre-processing are shown in Fig.8.

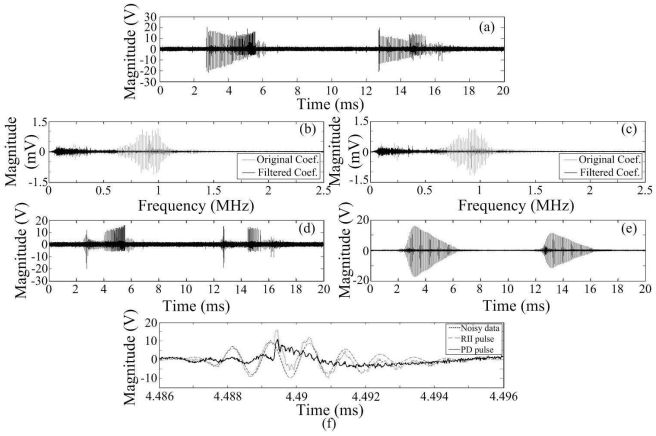

Fig. 8 The noisy data and filtered result, (a) noisy data, (b) the real Fourier coefficients before and after filtering, (c) the imaginary Fourier coefficients before and after filtering, (d) PD-contained signal, (e) repetitive impulsive interferences (RII), (f) amplified single pulse

The frequency range of PD is up to 15MHz as in Fig.5. But as illustrated in Fig. 8(b) and (c), most energy of the field-collected repetitive pulses concentrate around 1MHz. The two signals have overlapping frequency ranges. However, the repetitive pulses appear to be some singularities in Fourier coefficients that are totally different from PDs. Apparently, the large-amplitude coefficients in original data (gray coefficients in Fig.8(b) and (c)) are removed. Since this filtering method processes signal in pure frequency domain, it can effectively separate PD pulse and impulsive interference which occur at the same time. In Fig.8(f), three pulses that occur at the same time are amplified to demonstrate the effectiveness of this method in separating PDs and interferences that happen simultaneously. The noisy pulse is combined by one pulse from convertor and one PD pulse. After filtering the Fourier coefficients, the PD pulse and noise pulse are successfully separated.

The filtered data in Fig.8(d) is then analyzed by PD extracting algorithm. The relative entropy σ_E and relative peak-frequency σ_F are scattered in Fig.9(b). Here, σ_E and σ_F are divided into ten intervals. Since most data points in the first interval of σ_E are zeros and the number is too larger than the others to plot all bars in a same figure clearly, the first bar of the histogram of σ_E is not shown in Fig.9(c). According to the histograms of σ_E and σ_F, two boundaries are selected. One is around 0.37 in σ_E and the other is about 0.256 in σ_F. Thus, four zones are divided in σ_E-σ_F plane.

The signals of each zones are recovered via inverse STFT and portrayed in Fig.9(e) to (h). The signals recovered with the points in zone 1 are PD signals. Fig.9(b) shows these PD pulses have larger σ_E and smaller σ_F as discussed in section VI.

The result of de-noising procedure shows that the proposed method is able to detect PD signal and separate it from noises.

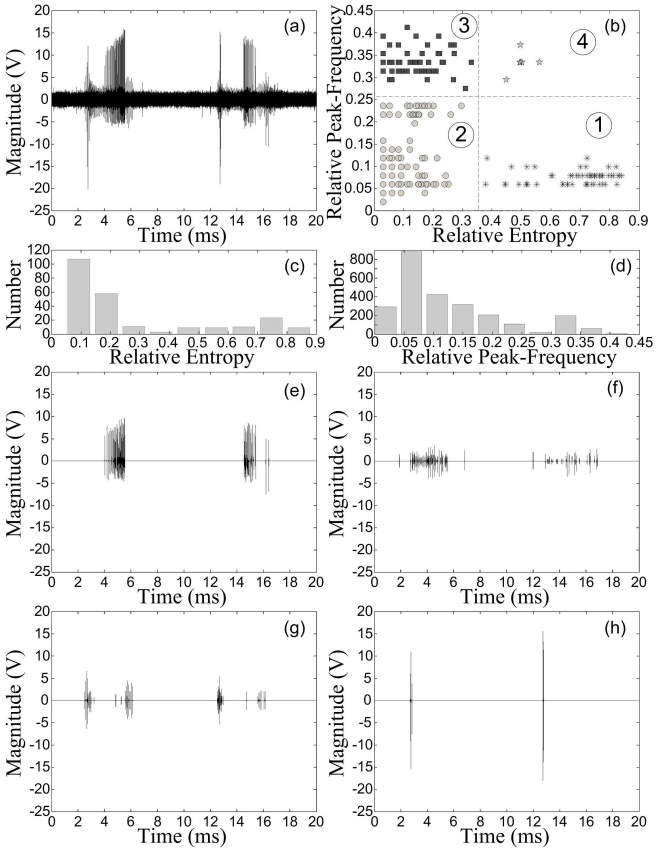

Fig. 9 Extracted PDs and noises, (a) filtered data, (b) σ_E-σ_F plane, (c) histogram of σ_E, (d) histogram of σ_F, (e)-(h) extracted pulse of each zone

VIII. Conclusion

Automatic PD extraction is realized in this paper through appropriate design of PD sensor and selection of suitable signal processing tools based on frequency distributions of PD pulses. According to the result of processing the combined noisy PD signal, this approach is capable of separating impulsive noises from PDs. Therefore, this advanced PD de-noising method can successfully supersede other existing PD de-noising methods in solving the problem of PD pulse extraction. It has several advantages over existing methods such as fast calculation and separating simultaneously-occurring pulses.

References

[1] M. D. Judd, O. Farish, J. S. Pearson and B. F. Hampton, "Dielectric windows for UHF partial discharge detection," IEEE Trans. Dielectrics and Electrical Insulation, vol. 8, pp. 953-958, 2001.

[2] P. Brown, "Nonintrusive partial discharge measurements on high voltage switchgear," in IEE Colloquium on Monitors and Condition Assessment Equipment (Digest No. 1996/186), 1996, pp. 10/1-10/5.

[3] Y. Li, Y. Wang, G. Lu, J. Wang, and J. Xiong, "Simulation of transient earth voltages aroused by partial discharge in switchgears," in 2010 Int. Conf. High Voltage Engineering and Application (ICHVE), 2010, pp. 309-312.

[4] R. Bartnikas, "Partial discharges. Their mechanism, detection and measurement," IEEE Trans. Dielectrics and Electrical Insulation, vol. 9, pp. 763-808, 2002.

[5] C. Caironi, D. Brie, L. Durantay and A. Rezzoug, "Interest and utility of time frequency and time scale transforms in the partial discharges analysis," in Conf. Record of the 2002 IEEE Int. Symp. Electrical Insulation, 2002, 2002, pp. 516-522.

[6] Y. H. M. Thayoob, Z. Zakaria, M. R. Samsudin, P. S. Ghosh, and M. L. Chai, "Preprocessing of acoustic emission signals from partial discharge in oil-pressboard insulation system," in 2010 IEEE Int. Conf. Power and Energy (PECon), 2010, pp. 29-34.

[7] K. L. Wong, "Electromagnetic emission based monitoring technique for polymer ZnO surge arresters," IEEE Trans. Dielectrics and Electrical Insulation, vol. 13, pp. 181-190, 2006.

[8] A. Cavallini, A. Contin, G. C. Montanari and F. Puletti, "Advanced PD inference in on-field measurements. Part I: Noise rejection," IEEE Trans. Dielectrics and Electrical Insulation, vol. 10, pp. 216-224, Apr 2003.

[9] H. Zhang, T. R. Blackburn, B. T. Phung and D. Sen, "A novel wavelet transform technique for on-line partial discharge measurements. Part 1: WT de-noising algorithm," IEEE Trans. Dielectrics and Electrical Insulation, vol. 14, pp. 3-14, Feb 2007.

[10] BSI, "High-Voltage Test Techniques - Partial Discharge Measurements," in IEC 60270, ed. London: European Committee for Electrotechnical Standardization, 2001, p. 7.

[11] S. G. Mallat, "Time Meets Frequency," in A Wavelet Tour of Signal Processing : The Sparse Way, Sparse ed Amsterdam ; Boston: Elsevier /Academic Press, 2009, pp. 89-150.

[12] D. L. Donoho and I. M. Johnstone, "Ideal spatial adaptation by wavelet shrinkage," Biometrika, vol. 81, pp. 425-455, Sep 1994.

[13] M. Misiti, Y. Misiti, G. Oppenheim and J.-M. Poggi. (1996). Wavelet Toolbox for Use with MATLAB: User's Guide (1st ed.).

[14] S. Verdú, S. W. McLaughlin and IEEE Information Theory Society., "Fifty Years of Shannon Theory," in Information theory 50 years of discovery, ed New York: IEEE Press, 2000.

Luo Guomin was born in Neijiang, China in 1983. She received the bachelor and master degree from Southwest Jiaotong University, China in 2005 and 2009, respectively. Now, she is a Ph.D student in Nanyang Technological University.

Zhang Daming received his bachelor's and master's degrees from Huazhong University of Science and Technological University in Years 1993 and 1996 respectively. He worked in Guoce Corporation, China from 1996 to 1997 as a design engineer. From 1999 to 2003, he was with Institute of High Performance Computing to carry out research on EMI/EMC. He then joined in Nanyang Technological University in May, 2003 as an assistant professor. Now he joins School of Electrical Engineering and Telecommunication in University of New South Wales.

Yong Kwee Koh, Kim Teck Ng, Helmi Kurniawan and Weng Hoe Leong are with Hoestar Inspection International Pte Ltd., Singapore.